

Thermal and mechanical response of [0001]-oriented GaN nanowires during tensile loading and unloading

Kwangsub Jung, Maenghyo Cho, and Min Zhou

Citation: *J. Appl. Phys.* **112**, 083522 (2012); doi: 10.1063/1.4759282

View online: <http://dx.doi.org/10.1063/1.4759282>

View Table of Contents: <http://jap.aip.org/resource/1/JAPIAU/v112/i8>

Published by the [American Institute of Physics](#).

Related Articles

Combined effect of nanoscale grain size and porosity on lattice thermal conductivity of bismuth-telluride-based bulk alloys

J. Appl. Phys. **112**, 084315 (2012)

Dynamical thermal conductivity of bulk semiconductor crystals

J. Appl. Phys. **112**, 083515 (2012)

Measurement setup for the simultaneous determination of diffusivity and Seebeck coefficient in a multi-anvil apparatus

Rev. Sci. Instrum. **83**, 093903 (2012)

Effective thermal conductivity of graphene-based composites

Appl. Phys. Lett. **101**, 121916 (2012)

Assessment of phonon boundary scattering from light scattering standpoint

J. Appl. Phys. **112**, 063513 (2012)

Additional information on *J. Appl. Phys.*


Journal Homepage: <http://jap.aip.org/>

Journal Information: http://jap.aip.org/about/about_the_journal

Top downloads: http://jap.aip.org/features/most_downloaded

Information for Authors: <http://jap.aip.org/authors>

ADVERTISEMENT



Special Topic Section:
PHYSICS OF CANCER

Why cancer? Why physics? [View Articles Now](#)

Thermal and mechanical response of [0001]-oriented GaN nanowires during tensile loading and unloading

Kwangsub Jung,¹ Maenghyo Cho,¹ and Min Zhou^{1,2,a)}

¹*Division of Multiscale Mechanical Design, School of Mechanical and Aerospace Engineering, Seoul National University, Seoul 151-742, South Korea*

²*George W. Woodruff School of Mechanical Engineering, Georgia Institute of Technology, Atlanta, Georgia 30332, USA*

(Received 14 June 2012; accepted 25 September 2012; published online 23 October 2012)

Molecular dynamics simulations are carried out to investigate the thermal and mechanical responses of GaN nanowires with the [0001] orientation and hexagonal cross sections to tensile loading and unloading. The thermal conductivity of the nanowires at each deformed state is calculated using the Green-Kubo approach with quantum correction. The thermal conductivity is found to be dependent on the strain induced by tensile loading and unloading. Phase transformations are observed in both the loading and unloading processes. Specifically, the initially wurtzite-structured (WZ) nanowires transform into a tetragonal structure (TS) under tensile loading and revert to the WZ structure in the unloading process. In this reverse transformation from TS to WZ, transitional states are observed. In the intermediate states, the nanowires consist of both TS regions and WZ regions. For particular sizes, the nanowires are divided into two WZ domains by an inversion domain boundary (IDB). The thermal conductivity in the intermediate states is approximately 30% lower than those in the WZ structure because of the lower phonon group velocity in the intermediate states. Significant effects of size and crystal structure on mechanical and thermal behaviors are also observed. Specifically, as the diameter increases from 2.26 to 4.85 nm, the thermal conductivity increases by 30%, 10%, and 50%, respectively, for the WZ, WZ-TS, and WZ-IDB structured wires. However, change in conductivity is negligible for TS-structured wires as the diameter changes. The different trends in thermal conductivity appear to result from changes in the group velocity which is related to the stiffness of the wires and surface scattering of phonons. © 2012 American Institute of Physics. [<http://dx.doi.org/10.1063/1.4759282>]

I. INTRODUCTION

Gallium nitride is a semiconducting material with many advantages. It has a number of potential applications in high-temperature electronic devices because of its wide bandgap energy and stability at high temperatures.^{1–5} It is also known to be piezoelectric like other semiconducting materials,⁶ such as ZnO, AlN, CdS, and BaTiO₃. Recently, the coupled piezoelectric and semiconducting properties of nanowires and nanorods led to the development of nanopiezotronics,⁷ which are expected to be used in a wide range of applications for flexible nanoelectronic devices, multifunctional nanosystems, and self-powered nanodevices.^{8–10}

The wurtzite (WZ) structure of semiconducting materials like GaN, ZnO, and CdS may transform into a tetragonal structure (TS),^{11,12} rocksalt structure^{13,14} or graphite-like structure (HX)^{15,16} in response to loading along different crystalline directions. These phase transformations cause changes in thermal response as well as the mechanical response. The design of flexible nanodevices using WZ-structured semiconductor nanowires may take advantage of a combination of mechanical and thermal responses. The phase transformation from WZ to HX observed in [01 $\bar{1}$ 0]-oriented ZnO nanowires under tensile loading is one exam-

ple.^{15,16} Thermal conductivity of the ZnO nanowires increases during the transformation from WZ to HX because the density of the HX structure is higher than that of the WZ structure.¹⁶ In our previous work,¹⁷ a phase transformation from WZ to TS structure is shown to occur in [0001]-oriented GaN nanowires under tensile loading. In contrast to what is observed in the [01 $\bar{1}$ 0]-oriented ZnO nanowires, the phase transformation from WZ to TS lowers the thermal conductivity of the GaN nanowires. The density of the TS structure is almost the same as that of the WZ structure,¹¹ but a surface layer with a structure different from the TS structure in the interior of the transformed nanowires causes the thermal conductivity to be lower.¹⁷ During the WZ-to-HX transformation, nanowires consist of both WZ regions and HX regions. Wires in the intermediate states have thermal conductivities that decrease due to the formation of the interfaces first and increase with the progress of transformation because the fraction of atoms in the HX phase increases.¹⁶ Such intermediate states are not observed for GaN and, consequently, the change in thermal conductivity is not significant during the transformation from WZ to TS under tensile loading.¹⁷ However, the intermediate states are observed during the reverse transformation from TS to WZ during unloading of transformed GaN nanowires. In this work, we analyze and compare the mechanical and thermal responses of GaN nanowires associated with both the forward transformation during loading and the reverse transformation during

^{a)}Electronic mail: min.zhou@gatech.edu. Tel: 404-894-3294. Fax: 404-894-0186.

unloading using molecular dynamics (MD) simulations. The effects of strain, structural change, and size on thermal conductivity are delineated.

II. METHODS

The GaN nanowires considered are shown in Fig. 1. The axis of the nanowires is oriented in the [0001] crystalline direction. Initially, Ga and N atoms are arrayed in a single-crystalline WZ structure. Periodic boundary conditions are used along the axial direction. The length of the periodic computational cell is 14.45 nm, which is sufficient to avoid image effects.¹⁸ The nanowires have hexagonal cross-sections with a six-fold symmetry and $\{01\bar{1}0\}$ lateral surfaces. Such shapes are observed in GaN nanowires grown by metalorganic chemical vapor deposition.¹⁹ Five diameters (2.26, 2.91, 3.55, 4.20, and 4.85 nm) are considered so the size effect can be outlined. The relatively small diameters considered highlights the effect of surfaces on the thermal and mechanical behaviors of the nanowires. MD simulations are carried out using the LAMMPS code.²⁰ Temperature is controlled by using the Nosé-Hoover method.²¹ The short-range interactions between atoms are described by using the Buckingham potential²² and the long-range Coulombic forces are evaluated by using the Wolf summation.^{23,24} The nanowires are equilibrated for 100 ps without any external load by using an NPT (isothermal-isobaric ensemble (constant temperature and constant pressure ensemble)) algorithm before deformations under tensile and compressive loading. After the equilibration, deformations of the nanowires are analyzed using a quasi-static loading scheme with a strain rate of 0.05 ns^{-1} . Each loading and unloading step involves a strain increment of $\pm 0.2\%$ and an equilibration period of 40 ps per with an NVT ensemble (canonical ensemble). Unloading of the nanowires is carried out from a strain of 0.1.

To investigate the effect of mechanical deformation, the thermal responses of the nanowires are determined as a function of strain. The thermal conductivity in the axis direction at each strain is evaluated by using the equilibrium Green-Kubo method.²⁵ The heat flux at each strain is calculated over a period of 500 ps in NVE ensemble (microcanonical ensemble). The thermal conductivity κ is calculated by using the relation

$$\kappa = \frac{1}{Vk_B T^2} \int_0^\infty \langle J(0) \cdot J(t) \rangle dt, \quad (1)$$

where V is the volume of the nanowire, k_B is the Boltzmann constant, T is the temperature, $\langle J(0) \cdot J(t) \rangle$ is the heat current

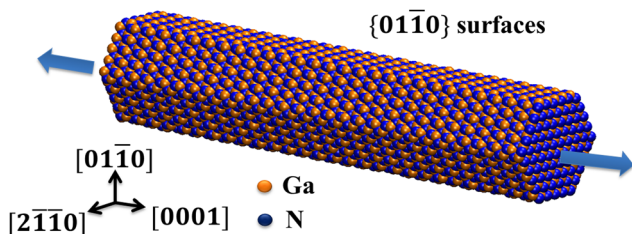


FIG. 1. [0001]-oriented GaN nanowire with the wurtzite structure and a hexagonal cross section.

autocorrelation function. The integral is truncated after a delay time τ_m . At this delay time, the system is assumed to have reached equilibrium. The average value over the delay time range of $2 < \tau_m < 5 \text{ ps}$ is taken as the thermal conductivity. Longer delay time reduces the number of time origins available for averaging, causing statistical errors to increase. The thermal conductivity values are averages of at least five simulations which are different only in initial random realization of atomic velocities. The thermal conductivity of bulk WZ GaN calculated by using the same method is 145 W/mK . This value is within the range of the experimental results of $125\text{--}230 \text{ W/mK}$.^{26–29} The simulations are performed at a constant temperature of 300 K, below the Debye temperature of GaN. Quantum corrections³⁰ are applied to temperature and thermal conductivities. The temperature calculated using MD is 477.1 K and the corresponding quantum-corrected temperature is 300 K.¹⁷

III. RESULTS

The mechanical behaviors of the nanowires during loading and unloading are analyzed first. Figure 2(a) shows stress as a function of strain for the nanowires with a diameter of 2.91 nm. Under tensile loading, the WZ-structured nanowires stretch and the stress increases steadily from point A to B along the solid red line of Fig. 2(a) as the strain increases from zero to 0.06. When the WZ structure transforms to TS structure at the strain of 0.06, the stress drops from 18.8 to 4.6 GPa precipitously (B-C). The transformation occurs through a combination of the breaking and formation of

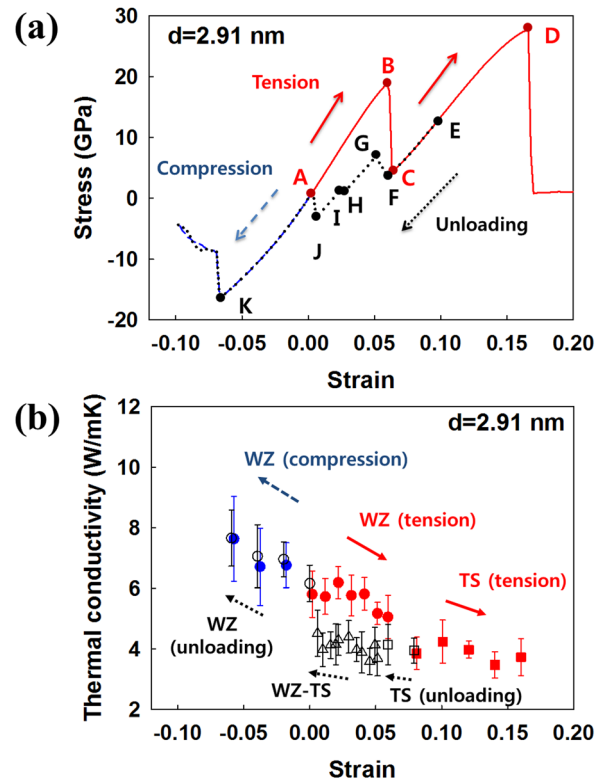


FIG. 2. (a) Stress as a function of strain for a nanowire with diameter $d=2.91 \text{ nm}$. (b) Thermal conductivity as a function of strain for the same nanowire. Error bars denote standard deviation of conductivity.

cation-anion bond along the $[0001]$ direction.¹¹ After the transformation, the nanowires deform elastically in the TS structure (C-D) and break into two pieces at the second drop in stress at the strain of 0.17. The failure strain and failure stress are very high, because the nanowires are very small in diameter and do not contain defects. The atomic arrangement on the $(01\bar{1}0)$ cross-section is shown in Fig. 3. The transformed nanowires have a surface layer whose structure is different from the TS structure in the interior as shown in Fig. 3(b). The stress-strain response for the unloading process is shown with the black dotted line in Fig. 2(a). Unloading from the strain of 0.1 is first associated with the recovery of the elastic deformation within the TS structure (E-F). A reverse transformation from TS to WZ initiates at the strain of 0.05 (F-G). During the reverse transformation, the nanowires consist of both TS-structured regions and WZ-structured regions as shown in Figs. 3(c) and 3(d). Two different stages are observed in the TS-to-WZ transformation. As seen in Fig. 3(c), the parts of the wires close to the surfaces transform to the WZ structure (G-H). In the next stage, the core of the nanowires transforms from TS to WZ, as shown in Fig. 3(d) (I-J). The reverse transformation completes at zero strain and the unloading path from point A in Fig. 2(a) coincides with that of the compression of a fresh, initially WZ-structured nanowires. Under compressive loading, similar elastic deformation in the WZ-structure occurs through the compression of the nanowires. For bulk GaN, the transformation from WZ to TS and the reverse transformation from TS to WZ are also observed. However, the WZ structure transforms into the HX structure under uniaxial compression along the $[0001]$ direction,¹⁴ but such transformation is not observed in the nanowires. The reason is that the critical stress for WZ-to-HX transformation is -30.5 GPa,¹⁵ but buckling occurs at the stress of -16.1 GPa for the nanowires here. The phase transformations are also observed for strain rates as low as 0.002 ns⁻¹, which corresponds to an equilibration period of 1 ns.

Figure 2(b) shows the thermal conductivity as a function of strain for the nanowires in Fig. 2(a) (diameter $d=2.91$ nm). The thermal conductivity decreases from its initial value of 5.8 W/mK by 13% as the strain increases to 0.06. Under compression, the thermal conductivity increases from the initial value by 31% as the strain decreases to -0.06 . The thermal conductivity decreases as the strain increases, and increases as the strain decreases.³¹ This trend in thermal conductivity comes from the dependence of phonon relaxation time on strain.^{32,33} Specifically, the relaxation time decreases when the strain changes from compression to tension. The thermal conductivity of the TS-structured nanowires with a strain of 0.1 is 4.2 W/mK which is 27% lower than that of the unstressed WZ nanowires. The decrease in conductivity is attributed to the strain of the wire and a higher disorder in the surface of the TS-structured wires than that of the WZ-structured wire,¹⁷ as illustrated in Fig. 3. In the unloading process, thermal conductivities of the WZ-structured nanowires and the TS-structured nanowires are similar to those in the loading process at each strain. However, the thermal conductivities of the nanowires in the intermediate states of the reverse transformation are lower than those of the WZ-structured nanowires under loading. At strain of 0.01, the thermal conductivity at the intermediate state is 4.0 W/mK, which is 31% lower than that of the WZ-structured nanowires. The dominant contribution causing the thermal conductivity at the intermediate state to be lower than that of the WZ-structured nanowires arises from the phonon group velocity. The thermal conductivity is known to be related to the phonon group velocity and the relaxation time of phonons.³⁴ At the strain of 0.01, the elastic modulus of the nanowires in the intermediate state is 206 GPa, which is 37% lower than that of the WZ-structured nanowires and causes the group velocity to be approximately 20% lower. However, the average relaxation time of phonons in the intermediate state is very similar to that for the WZ-structured nanowires. At the completion of the reverse transformation

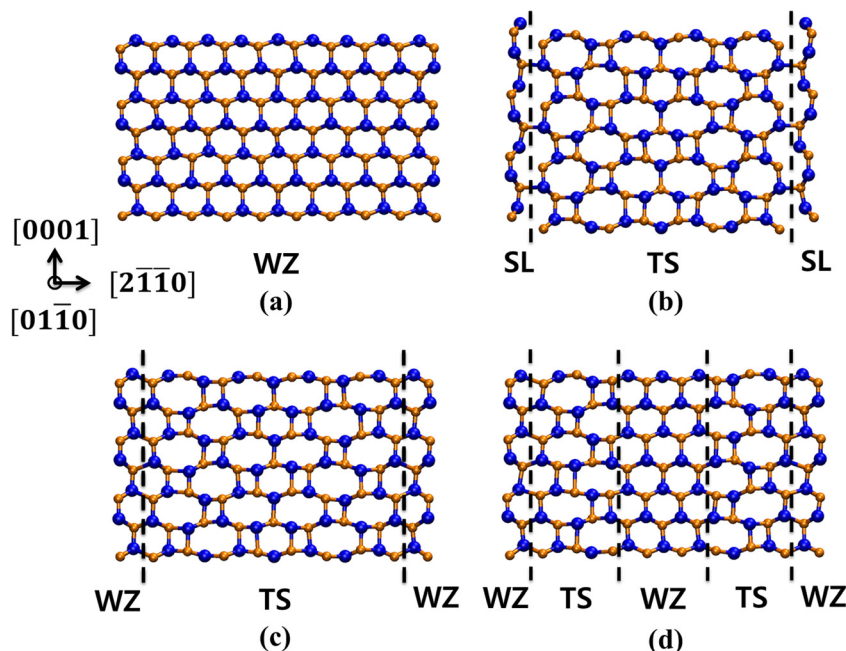


FIG. 3. Atomistic arrangements on $(01\bar{1}0)$ cross-sections of a nanowire with $d=2.91$ nm under tensile loading and unloading: (a) WZ-structured wire at zero strain; (b) TS-structured wire at a strain of 0.1; (c) WZ-TS structured wire at a strain of 0.04; and (d) WZ-TS structured wire at a strain of 0.02.

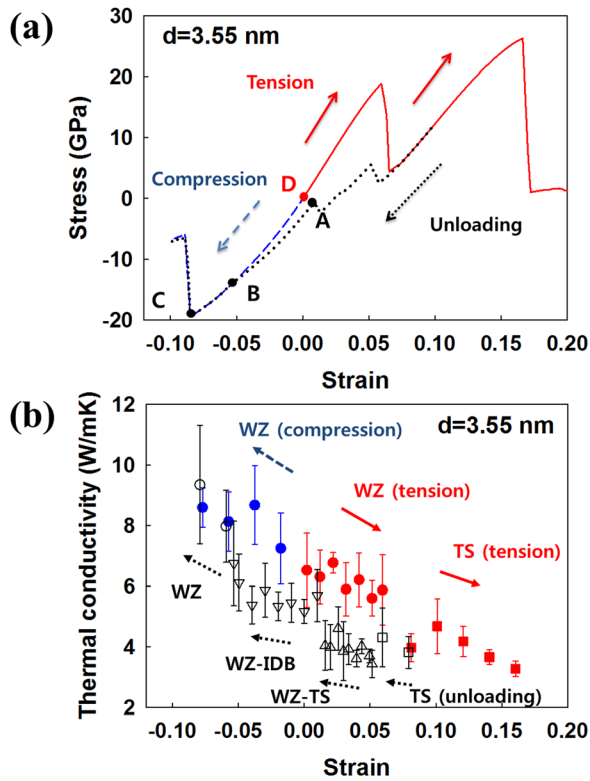


FIG. 4. (a) Stress as a function of strain for a nanowire with diameter $d=3.55$ nm. (b) Thermal conductivity as a function of strain for the same nanowire. Error bars denote standard deviation of conductivity.

from TS to WZ, the thermal conductivity increases by 55% and the stiffness increases by 54% as the strain decreases from 0.01 to zero. Such changes in conductivity are not observed at the completion of the WZ-to-HX transformation in ZnO nanowires.¹⁶ The thermal conductivity in ZnO nanowires increases when the fraction of HX exceeds that of WZ. Such changes in conductivity and fractions are gradual and steady. Dominant effects that cause the thermal conductivity to increase during the WZ-to-HX transformation come from the higher density of HX compared with that of WZ. However, the density of the TS structure is almost the same as

that of WZ.¹¹ In the TS-to-WZ transformation, the Young's modulus of the nanowires contributes to the change in thermal conductivity.

The mechanical and thermal behaviors of the nanowires with a diameter of 3.55 nm are also analyzed. Under tensile loading, the mechanical response of the WZ-structured nanowires is similar to that of the nanowires with a diameter of 2.91 nm, as shown in Fig. 4(a). A similar phase transformation from WZ to TS is also observed, as seen in Fig. 5. The same reverse transformation from TS to WZ is observed as well in the unloading process. However, the TS-to-WZ transformation does not complete at zero strain and the unloading path from point A to point B in Fig. 4(a) does not coincide with the compression path of the original WZ-structured nanowires from point D to point B. The reason is that the thicker nanowire is divided into two WZ domains, as shown in Fig. 5(d). The polarity of the core domain is opposite to that of the outer domain. The boundary between the two domains is an inversion domain boundary (IDB).^{35,36} Similar IDBs have been observed in experiments³⁵ and MD simulations³⁷ of GaN nanorods. The mechanical and thermal responses are also affected by the existence of the IDB. The stiffness of the nanowires with the IDB is 16% lower than that of the WZ-structured nanowires, causing the thermal conductivity to be 21% lower. Such structure is not observed in the nanowires with a diameter of 2.91 nm. The formation of the IDB during the reverse transformation is dependent on the lateral size of the nanowire. As shown in Fig. 5, the nanowires with the diameter of 3.55 nm have six layers of atoms from the surfaces to the core. In the WZ-structured wires, all layers have same sequence of Ga and N atoms along the axis. In Fig. 5(a), the third and fifth layers from the surfaces change their polarity and the WZ structure transforms to the TS. During reverse transformation, the sixth layers (the first from the core) change the polarity and the WZ structures appear in the core of the wires in Fig. 5(c), and polarity change in the fourth layers forms the IDB between the surface layers (the first and second layers) and the core layers (from the third to sixth). However, for the nanowires with

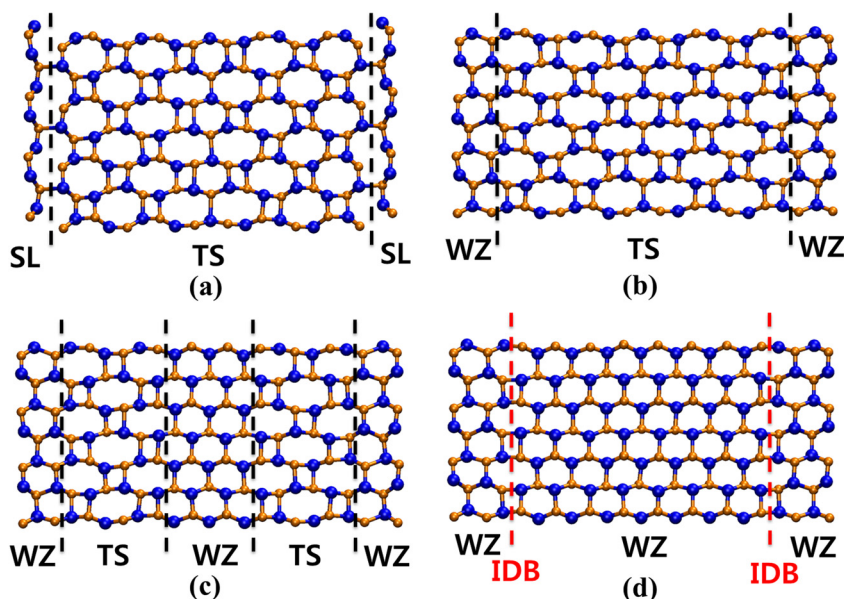


FIG. 5. Atomistic arrangements on $(01\bar{1}0)$ cross-sections of a nanowire with $d=3.55$ nm during the transformation from TS to WZ during unloading: (a) TS-structured wire at a strain of 0.1; (b) WZ-TS structured wire at a strain of 0.04; (c) WZ-TS structured wire at a strain of 0.02; and (d) WZ-IDB structured wire at zero strain.

the diameter of 2.91 nm and five layers of atoms, the polarity of the third and fifth layers changes in the forward transformation, and is restored to the initial direction during the reverse transformation. The difference in the number of layers between the two cases is the major factor in the formation of the IDB in the TS-to-WZ transformation. The IDB structure is observed in the nanowires with even number of layers ($d = 2.26, 3.55, \text{ and } 4.85 \text{ nm}$), but not in the nanowires with odd number of layers ($d = 2.91 \text{ and } 4.20 \text{ nm}$).

The effect of size on the mechanical and thermal responses is analyzed. Figure 6 compares the stress-strain curves for nanowires with different diameters. The stress-strain response is dependent on the wire size and atomistic structure. As the diameter increases from 2.26 to 4.85 nm, the failure strength decreases from 30.6 to 24.6 GPa and the critical stress required for the initiation of the reverse transformation from TS to WZ decreases from 5.2 to 1.4 GPa, as shown in Fig. 7 and Table I. However, such a significant change is not observed in the critical stress required for the WZ-to-TS transformation under tensile loading over the same range of diameters. For bulk GaN, critical stresses for transformation from WZ to TS, breaking, transformation from TS to WZ are 19.0 GPa, 15.5 GPa, and -6.8 GPa , respectively. These values are consistent with the trends in the size effect seen for the nanowires. The above trends are related to the elastic moduli of the nanowires. Figure 8 and Table II show the elastic moduli of the nanowires with different atomistic structures. Over the range of diameters from

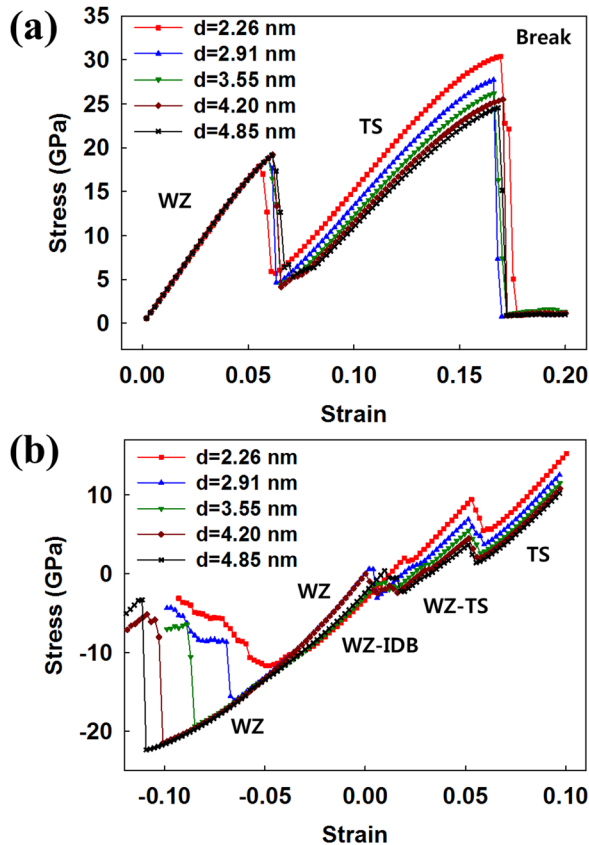


FIG. 6. Stress as a function of strain for nanowires with diameters of 2.26, 2.91, 3.55, 4.20, and 4.85 nm: (a) under tensile loading; and (b) during unloading.

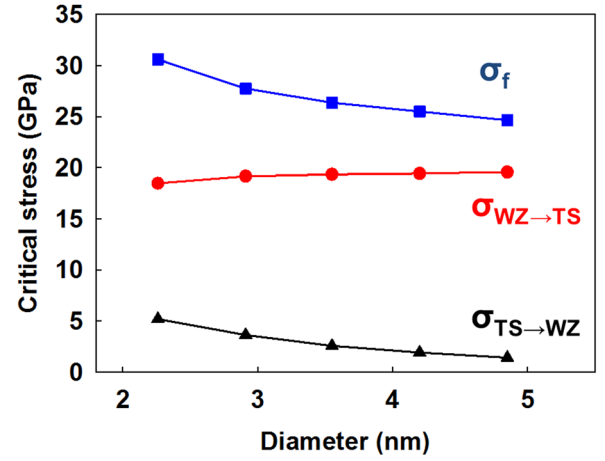


FIG. 7. Critical stresses for breaking (σ_f), phase transformation from WZ to TS ($\sigma_{WZ \rightarrow TS}$), and reverse transformation from TS to WZ ($\sigma_{TS \rightarrow WZ}$) as functions of wire diameter in the range from 2.26 nm to 4.85 nm.

2.26 to 4.85 nm, the elastic moduli of the TS-structured nanowires at the strain of 0.1 and the WZ-TS structured nanowires at the strain of 0.04 decrease by 13% and 32%, respectively. The decrease in moduli is also indicated by the slopes of the stress-strain curve in Fig. 6. For the ZnO wires with both WZ and TS structures, the modulus shows very similar size dependence,¹² caused by the high surface-to-volume ratio and the tensile surface stress. On the other hand, such significant size dependence is not observed for the WZ-structured GaN nanowires. Because the stiffness of ZnO is lower than that of GaN, surface stresses play a more significant role in ZnO, causing the size effect to be more pronounced in the ZnO nanowire.^{38,39}

The thermal conductivities of the nanowires of WZ, TS, WZ-TS, and WZ-IDB structures are shown as functions of wire diameter in Fig. 9. Detailed results are listed in Table III. The difference in size effect on the mechanical properties results in different trends in thermal conductivity among the wires of the different atomistic structures. The thermal conductivity increases by 30%, 10%, and 50%, respectively, for the unstressed WZ-structured, WZ-TS structured, and WZ-IDB structured wires over the size range analyzed. From the kinetic theory, thermal conductivity can be reduced to a simple expression

$$\kappa = Cv^2\tau, \quad (2)$$

TABLE I. Critical stresses for transformation from WZ to TS, breaking, transformation from TS to WZ, and buckling and critical strains of the nanowires analyzed and for bulk GaN.

Diameter (nm)	2.26	2.91	3.55	4.20	4.85	Bulk
$\sigma_{WZ \rightarrow TS}$ (GPa)	18.5	19.2	19.4	19.4	19.6	19.0
$\epsilon_{WZ \rightarrow TS}$ (%)	5.8	6.1	6.2	6.3	6.4	6.9
σ_f (GPa)	30.6	27.8	26.4	25.5	24.6	15.5
ϵ_f (%)	17.3	16.6	16.8	17.1	16.9	13.5
$\sigma_{TS \rightarrow WZ}$ (GPa)	5.2	3.6	2.6	1.9	1.4	-6.8
$\epsilon_{TS \rightarrow WZ}$ (%)	5.9	5.8	5.7	5.6	5.5	1.2
$\sigma_{buckling}$ (GPa)	-11.7	-16.1	-19.4	-21.5	-22.4	...
$\epsilon_{buckling}$ (%)	-4.4	-6.5	-8.5	-10.1	-10.9	...

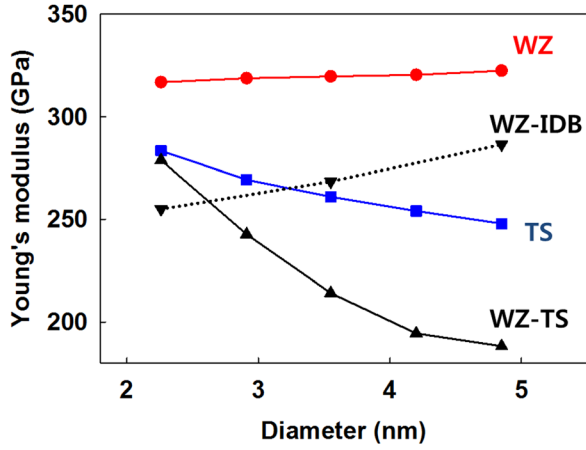


FIG. 8. Elastic moduli of WZ-structured, TS-structured, WZ-TS structured, and WZ-IDB structured nanowires as functions of diameter.

where C , v , and τ are heat capacity per unit volume, group velocity of phonons, and relaxation time of phonons, respectively. The crossover from diffusive to ballistic transport in nanowires may occur at a distance shorter than 10 nm.⁴⁰ Phonon transport in the nanowires analyzed are diffusive transport because the length of the nanowires is 14.45 nm. We estimate the phonon relaxation time by calculating an average decay time of heat current

$$\tau_{av} = \frac{V\kappa k_B T^2}{\langle J(0) \cdot J(0) \rangle}, \quad (3)$$

because the relaxation time of the heat current is very similar to that of phonons.⁴¹ In Fig. 10, the relaxation times of the nanowires increases by 30%, 10%, 30%, and 60%, respectively, for the WZ, TS, WZ-TS, and WZ-IDB wires. At the same zero strain, the relaxation time of the WZ wires is very similar to that of the WZ-IDB wires over the range of the wire size shown. Because the surface structures of WZ, WZ-TS, and WZ-IDB wires are almost the same as that of the WZ-structured wires, as shown in Figs. 3 and 5, the influence of surface scattering^{42–44} on the relaxation time of phonons is not different for the three types of wires. The difference in the relaxation time between the WZ wires and WZ-TS wires comes from the strain dependence of the relaxation time.³² At the same strain of 0.04, the relaxation times of both WZ and WZ-TS wires are within 10% of each other. The difference in conductivities between the wires with different structures results from the stiffness, which is related to the phonon group velocity.³⁴ This velocity is estimated simply

TABLE II. Elastic moduli of WZ-structured, TS-structured, WZ-TS structured, and WZ-IDB structured nanowires at strains of zero, 0.1, 0.04, and zero, respectively.

Diameter (nm)	2.26	2.91	3.55	4.20	4.85
E_{WZ} (GPa)	316.9	318.8	319.7	320.5	322.5
E_{TS} (GPa)	283.5	269.3	261.0	254.1	247.9
E_{WZ-TS} (GPa)	278.8	242.7	214.1	194.4	188.2
E_{WZ-IDB} (GPa)	255.0	...	268.5	...	286.5

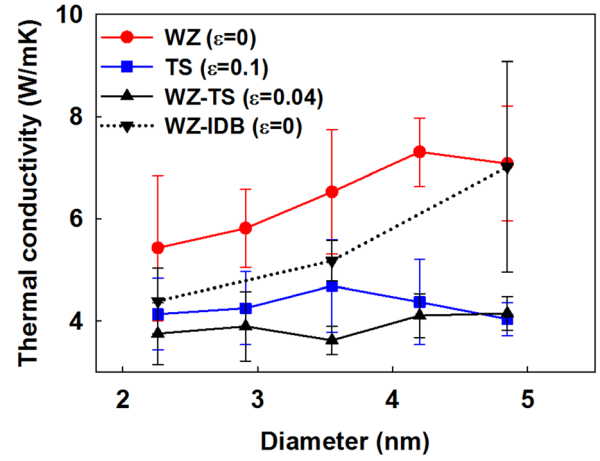


FIG. 9. Thermal conductivities in WZ-structured, TS-structured, WZ-TS structured, and WZ-IDB structured nanowires as functions of diameter. Error bars denote standard deviation.

by calculating a harmonic average over the longitudinal and transverse sound velocities,^{45,46} $v_L = \sqrt{C_{33}/\rho}$ and $v_T = \sqrt{C_{44}/\rho}$, respectively, where ρ is the mass density and C_{33} and C_{44} are elastic constants.⁴⁷ The estimated values of the group velocity are shown in Fig. 11. The thermal conductivity of the WZ wires is higher than that for the WZ-IDB wires due to the larger phonon group velocity of the WZ wires. However, for both the WZ and WZ-IDB wires, the size dependence of conductivity comes from the increase in the phonon relaxation time⁴⁸ because the change in group velocity is very small. For the WZ-TS structured wires, the decrease in group velocity reduces the effect of relaxation time, resulting in the small amount of increase in conductivity. However, thermal conductivity in the TS-structured wires does not show a significant change over the range of the wire size as shown in Fig. 9. The group velocity of the TS-structured wires with the diameter of 4.85 nm is larger than that of the WZ-TS structured wires with the same size, but corresponding thermal conductivities are almost same. Because the atomic arrangement on the surfaces of the TS-structured wires is different from that in the core, surface scatter of phonons is more pronounced for the TS-structured wires than other wires.¹⁷ As a result, the thermal conductivity in the TS-structured wires remains almost unchanged as the size increases.

IV. SUMMARY

The mechanical and thermal behaviors of [0001]-oriented GaN nanowires under tensile loading and unloading

TABLE III. Thermal conductivities of WZ-structured, TS-structured, WZ-TS structured, and WZ-IDB structured nanowires at strains of zero, 0.1, 0.04, and zero, respectively.

Diameter (nm)	2.26	2.91	3.55	4.20	4.85
κ_{WZ} (W/mK)	5.4	5.8	6.5	7.3	7.1
κ_{TS} (W/mK)	4.1	4.2	4.7	4.4	4.0
κ_{WZ-TS} (W/mK)	3.8	3.9	3.6	4.1	4.2
κ_{WZ-IDB} (W/mK)	4.7	...	5.2	...	7.0

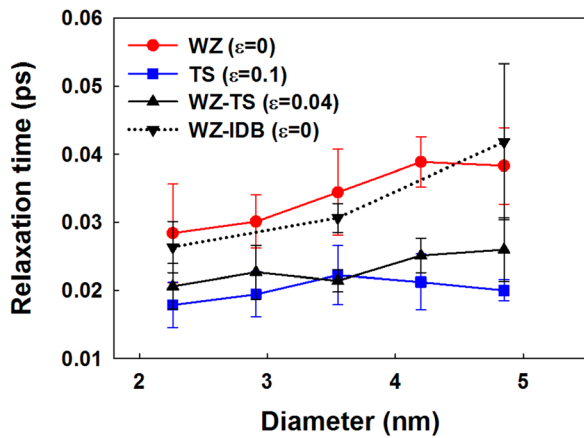


FIG. 10. Relaxation times for WZ-structured, TS-structured, WZ-TS structured, and WZ-IDB structured nanowires as functions of diameter. Error bars denote standard deviation.

are analyzed through molecular dynamics simulations. The thermal conductivity decreases as strain increases under tensile loading, and increases as strain decreases in the unloading process. The effect of strain on the conductivity comes from the change in the relaxation time of phonons. A reverse transformation from TS to WZ occurs during unloading. During the reverse transformation, the nanowires consist of both WZ-structured regions and TS regions. For the nanowires with diameters of 2.26, 3.55, and 4.85 nm, the formation of an IDB between two WZ domains is observed along the wire axis during the reverse transformation. Such intermediate states are not observed in the process of the forward transformation under tensile loading. Results show that the thermal conductivity is dependent on the lateral size and structural evolution of wires. The thermal conductivity increases by 30%, 10%, and 50%, respectively, for the WZ, WZ-TS, and WZ-IDB structured wires as the diameter increases from 2.26 to 4.85 nm, but the conductivity of the TS-structured wires does not change with the size. This effect is attributed to the phonon relaxation time and the mechanical behaviors of nanowires. The decrease in the elastic modulus of WZ-TS structured wires reduces the effect of

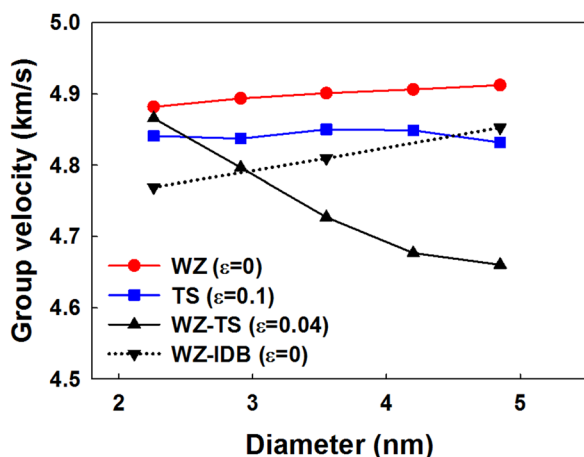


FIG. 11. Phonon group velocities for WZ-structured, TS-structured, WZ-TS structured, and WZ-IDB structured nanowires as functions of wire diameter.

phonon relaxation time by decreasing the group velocity. For the WZ and WZ-IDB structured wires, relaxation time of phonon is dominant factor for the conductivity increasing because change in group velocity is negligible for the range of size considered here. The dependence of thermal conductivity on the structure of nanowires results from the dependence of phonon group velocity on the structure of the nanowires.

ACKNOWLEDGMENTS

The authors gratefully acknowledge support from the National Research Foundation of Korea through the WCU (World Class University) program (Grant No. R31-2011-000-10083-0) at Seoul National University.

- ¹S. J. Pearton, F. Ren, A. P. Zhang, G. Dang, X. A. Cao, K. P. Lee, H. Cho, B. P. Gila, J. W. Johnson, C. Monier, C. R. Abernathy, J. Han, A. G. Baca, J. I. Chyi, C. M. Lee, T. E. Nee, C. C. Chuo, and S. N. G. Chu, *Mater. Sci. Eng., B* **82**, 227 (2001).
- ²J. Goldberger, R. He, Y. Zhang, S. Lee, H. Yan, H. Choi, and P. Yang, *Nature (London)* **422**, 599 (2003).
- ³S. Gradečak, F. Qian, Y. Li, H. Park, and C. M. Lieber, *Appl. Phys. Lett.* **87**, 173111 (2005).
- ⁴Y. Huang, X. Duan, Y. Cui, and C. M. Lieber, *Nano Lett.* **2**, 101 (2002).
- ⁵J. C. Johnson, H. Choi, K. P. Knutsen, R. D. Schaller, P. Yang, and R. J. Saykally, *Nature Mater.* **1**, 106 (2002).
- ⁶V. N. Brudnyi, A. V. Kosobutsky, and N. G. Kolin, *Phys. Solid State* **53**, 679 (2011).
- ⁷Z. L. Wang, *Adv. Mater.* **19**, 889 (2007).
- ⁸S. Xu, Y. Qin, C. Xu, Y. Wei, R. Yang, and Z. L. Wang, *Nat. Nanotechnol.* **5**, 366 (2010).
- ⁹M. Y. Choi, D. Choi, M. J. Jin, I. Kim, S. H. Kim, J. Y. Choi, S. Y. Lee, J. M. Kim, and S. W. Kim, *Adv. Mater.* **21**, 2185 (2009).
- ¹⁰G. Zhu, R. Yang, S. Wang, and Z. L. Wang, *Nano Lett.* **10**, 3151 (2010).
- ¹¹J. Wang, A. J. Kulkarni, K. Sarasamak, S. Limpijumnong, F. J. Ke, and M. Zhou, *Phys. Rev. B* **76**, 172103 (2007).
- ¹²J. Wang, A. J. Kulkarni, F. J. Ke, Y. L. Bai, and M. Zhou, *Comput. Methods Appl. Mech. Eng.* **197**, 3182 (2008).
- ¹³A. Mujica, A. Rubio, A. Muñoz, and R. J. Needs, *Rev. Mod. Phys.* **75**, 863 (2003).
- ¹⁴K. Sarasamak, A. J. Kulkarni, M. Zhou, and S. Limpijumnong, *Phys. Rev. B* **77**, 024104 (2008).
- ¹⁵A. J. Kulkarni, M. Zhou, K. Sarasamak, and S. Limpijumnong, *Phys. Rev. Lett.* **97**, 105502 (2006).
- ¹⁶A. J. Kulkarni and M. Zhou, *Nanotechnology* **18**, 435706 (2007).
- ¹⁷K. Jung, M. Cho, and M. Zhou, *Appl. Phys. Lett.* **98**, 041909 (2011).
- ¹⁸A. J. Kulkarni and M. Zhou, *Appl. Phys. Lett.* **88**, 141921 (2006).
- ¹⁹S. D. Hersee, X. Sun, and X. Wang, *Nano Lett.* **6**, 1808 (2006).
- ²⁰S. J. Plimpton, *J. Comput. Phys.* **117**, 1 (1995).
- ²¹W. G. Hoover, *Phys. Rev. A* **31**, 1695 (1985).
- ²²P. Zapol, R. Pandey, and J. D. Gale, *J. Phys.: Condens. Matter* **9**, 9517 (1997).
- ²³D. Wolf, P. Keblinski, S. R. Phillpot, and J. Eggebrecht, *J. Chem. Phys.* **110**, 8254 (1999).
- ²⁴C. J. Fennell and J. D. Gezelter, *J. Chem. Phys.* **124**, 234104 (2006).
- ²⁵S. G. Volz and G. Chen, *Phys. Rev. B* **61**, 2651 (2000).
- ²⁶E. K. Sichel and J. I. Pankove, *J. Phys. Chem. Solids* **38**, 330 (1977).
- ²⁷G. A. Slack, L. J. Schowalter, D. Morelli, and J. J. A. Freitas, *J. Cryst. Growth* **246**, 287 (2002).
- ²⁸A. Jeżowski, P. Stachowiak, I. Grzegory, B. A. Danilchenko, and T. Paszkiewicz, *Phys. Status Solidi B* **240**, 447 (2003).
- ²⁹W. Liu and A. Balandin, *Appl. Phys. Lett.* **85**, 5230 (2004).
- ³⁰Y. H. Lee, R. Biswas, C. M. Soukoulis, C. Z. Wang, C. T. Chan, and K. M. Ho, *Phys. Rev. B* **43**, 6573 (1991).
- ³¹R. C. Picu, T. Borca-Tasciuc, and M. C. Pavel, *J. Appl. Phys.* **93**, 3535 (2003).
- ³²S. Bhowmick and V. B. Shenoy, *J. Chem. Phys.* **125**, 164513 (2006).
- ³³X. Li, K. Maute, M. L. Dunn, and R. Yang, *Phys. Rev. B* **81**, 245318 (2010).

- ³⁴M. C. Roufousse and R. Jeanloz, *J. Geophys. Res.* **88**, 7399, doi:10.1029/JB088iB09p07399 (1983).
- ³⁵L. T. Romano, J. E. Northrup, and M. A. O'Keefe, *Appl. Phys. Lett.* **69**, 2394 (1996).
- ³⁶V. Potin, G. Nouet, and P. Ruterana, *Appl. Phys. Lett.* **74**, 947 (1999).
- ³⁷P. Xiao, W. Wang, J. Wang, F. Ke, M. Zhou, and Y. Bai, *Appl. Phys. Lett.* **95**, 211907 (2009).
- ³⁸Z. Wang, X. Zu, L. Yang, F. Gao, and W. J. Weber, *Phys. Rev. B* **76**, 045310 (2007).
- ³⁹R. A. Bernal, R. Agrawal, B. Peng, K. A. Bertness, N. A. Sandford, A. V. Davydov, and H. D. Espinosa, *Nano Lett.* **11**, 548 (2011).
- ⁴⁰M. J. Gilbert, R. Akis, and D. K. Ferry, *J. Appl. Phys.* **98**, 094303 (2005).
- ⁴¹S. Volz, J. B. Saulnier, and M. Lallemand, *Phys. Rev. B* **54**, 340 (1996).
- ⁴²L. Shi, Q. Hao, C. Yu, N. Mingo, X. Kong, and Z. L. Wang, *Appl. Phys. Lett.* **84**, 2638 (2004).
- ⁴³A. L. Moore, M. T. Pettes, F. Zhou, and L. Shi, *J. Appl. Phys.* **106**, 034310 (2009).
- ⁴⁴F. Zhou, A. L. Moore, J. Bolinsson, A. Persson, L. Fröberg, M. T. Pettes, H. Kong, L. Rabenberg, P. Caroff, D. A. Stewart, N. Mingo, K. A. Dick, L. Samuelson, H. Linke, and L. Shi, *Phys. Rev. B* **83**, 205416 (2011).
- ⁴⁵C. Guthy, C. Y. Nam, and J. E. Fischer, *J. Appl. Phys.* **103**, 064319 (2008).
- ⁴⁶W. L. Liu and A. A. Balandin, *J. Appl. Phys.* **97**, 073710 (2005).
- ⁴⁷A. Polian, M. Grimsditch, and I. Grzegory, *J. Appl. Phys.* **79**, 3343 (1996).
- ⁴⁸D. Li, Y. Wu, P. Kim, L. Shi, P. Yang, and A. Majumdar, *Appl. Phys. Lett.* **83**, 2934 (2003).